Morphological Influence of Precursor Composition Characteristics During Ceramic Membrane Fabrication

Sushma Chakraborty
Indian Institute of Technology Guwahati
Ramagopal Uppaluri
Indian Institute of Technology Guwahati
Chandan Das (cdas@iitg.ac.in)
Indian Institute of Technology Guwahati

Research Article

Keywords: Low cost, ceramic membranes, kaolin, saw dust, pore size, porosity, empirical model

Posted Date: May 17th, 2021

DOI: https://doi.org/10.21203/rs.3.rs-526013/v1

Morphological Influence of Precursor Composition Characteristics during Ceramic Membrane Fabrication

Sushma Chakraborty, Ramagopal Uppaluri* and Chandan Das*

Department of Chemical Engineering, Indian Institute of Technology Guwahati, Guwahati, Assam, India

*Corresponding author(s)

Email: cdas@iitg.ac.in (C. Das); ramgopalu@iitg.ac.in (R.G.V.S. Uppaluri)

Phone+ :91 361 258 2268/2260;

Fax+ :91 361 258 2291

Abstract

In this work, the influence of inorganic low-cost precursor compositions (viz. kaolin, feldspar, saw dust, sodium metasilicate and boric acid) has been investigated on the morphological characteristics (such as average pore size and porosity) of the ceramic membranes that were fabricated using dry compaction method and saw dust as the pore forming agent. In order to do so, kaolin to feldspar ratio has been varied from 0.48 – 2.05 and binder composition has been varied from 10 – 15 wt.%. For an inorganic precursor formulation of kaolin 38.77 wt.%, feldspar 23.03 wt.%, saw dust 8.19 wt.%, sodium metasilicate 15 wt.% and boric acid 15 wt.%, the sub-micron range low-cost ceramic membranes (95.8 nm average pore size and 13.95% porosity) have been achieved as a key novelty. With minor variations in the precursor composition, the microfiltration membranes could be converted to ultrafiltration membranes without undergoing any complex surface reactions or polymeric coatings. An empirical model has been as well developed to quantify the variation of dependent variables on the membrane characteristics.

Keywords: Low cost; ceramic membranes; kaolin; saw dust; pore size; porosity; empirical model.

1. Introduction

The application of membranes have been widespread in variety of industries such as water treatment, food processing, air purification and to sort environmental issues (Buonomenna, 2013; Chakraborty et al., 2020a; Chakraborty et al., 2020b; Ciora and Liu, 2003; Issaoui and Limousy, 2019; Kumar et al., 2015; Nandi et al., 2010; Vasanth et al., 2013). With respect to its polymeric counterpart, ceramic membranes have better shelf life, higher chemical, mechanical and thermal stability, resistance to high pressure, lower energy consumption and

easy of cleaning (Dong et al., 2006; Mallada and Menéndez, 2008; Mestre et al., 2019). However, the major disadvantage concerning the application of ceramic membrane have been related to the higher cost associated with the precursor materials used for fabrication such as alumina, titania, zirconia, etc. and higher sintering temperatures (Abdullayev et al., 2019; DeFriend et al., 2003; Horri et al., 2012; Mingyi et al., 2010; Nandi et al., 2011; Wang et al., 2006). Hence, the main challenge towards effective exploitation of ceramic membranes lies in optimizing the cost of membrane precursor material and process parameters.

Due to this cost limitations, over the past few years, researches have been widely conducted to reduce the cost associated with the ceramic membranes by using low cost precursor materials such as natural clay, sawdust, fly ash, starch, kaolin, diatomite dolomite, rice husk, egg shell, etc. (Ha et al., 2015; Lorente-Ayza et al., 2015; Mohanta et al., 2014b; Obada et al., 2017; Xavier et al., 2019; Yang and Tsai, 2008).

With judicious use of precursor material, the cost of ceramic membranes may be reduced to a large extent without compromising its benefits in terms of performance and the benchmark set by the otherwise expensive commercially available ceramic membranes could be reached. Low cost ceramic membranes have been effectively utilized in the waste water treatment and food processing sectors, till date (Nandi et al., 2011; Qin et al., 2015; Vasanth et al., 2013). However, the major drawback of using the low cost precursor material are with membrane morphological characteristics since they possess higher pore size and porosities and produce non-uniformity in the structures. This disadvantage also restricts the commercial applications of low-cost ceramic membranes in most of the fields. Hence, efforts have been made in this work to develop ceramic membranes with better morphological characteristics. Nevertheless, ongoing efforts in low cost and conventional ceramic membrane research do not advocate upon systematic variation in precursor compositions to understand the underlying mechanisms and complex interaction associated to significant reduction in average membrane

pore size. Such investigations will be very useful to encourage process-product optimality from a combinatorial perspective.

In this article, emphasis has been given to develop low cost ceramic membranes with inexpensive precursor materials and bio pore-former with reduced average pore size and average porosity. The variation in membrane properties with the variation in precursor composition has been studied extensively. In order to quantify the influence of the raw materials used for fabrication, empirical models have also been developed for both the dependent variables with respect to alternate precursor composition.

2. Materials and Methods

2.1 Raw Materials

The raw materials used for the fabrication of ceramic membranes were kaolin, feldspar, boric acid, sodium metasilicate and sawdust. Feldspar was procured from National Chemicals (Gujarat. India); boric acid (purity: 99.5 %) was procured from Merck (India); and sodium metasilicate nonahydrate (purity: 95 %) and kaolin (pure) were purchased from Central Drug House (P) Ltd. (New Delhi, India). Sawdust which were used as natural bio pore-former, were prepared from wood flakes obtained from local furniture shops around IIT Guwahati campus.

2.2 Fabrication of Low Cost Ceramic Membranes

The low cost ceramic membranes were fabricated following the procedure adopted by Chakraborty et al. (2018) (Chakraborty et al., 2018). Firstly, the sawdust particles were sieved through 355 µm mesh sieves and the average particle size of the membranes were approximately 254 µm (Chakraborty et al.). Then, appropriate quantities of all the precursor materials (kaolin, feldspar, sodium metasilicate and boric acid) along with sawdust were mixed together in a mixer grinder in order to ensure uniform distribution of the components in the

mixture (Table 1). The concentration of saw dust was kept fixed at 8 wt.%. An important perception with respect to the targeted compositional variations is with respect to the emphasis on the ratio of kaolin to feldspar which was varied from about 0.48 to 2.05. This was targeted to achieve membranes with greater variation in the content of kaolin and feldspar. The value range of 0.48 to 2.05 was based on few trial and error investigations. The binder compositions (boric acid and sodium metasilicate) were varied from 10 – 15 wt.%. Ceramic membranes (disc-shaped) with diameter 5.5 cm and 5 mm thickness were then fabricated using stainless steel molds under 100 kgf/cm^2 pressure (for 2 min) using hydraulic press (Make: Velan Engineering, Tamilnadu, India). The disc-shaped structures were then subjected to heat treatment at 100 °C for 12 h and 250 °C for 24 h and finally sintered at 850 °C for 6 h. The heat treatment steps were carried out at a heating rate of 2 °C/min. The ceramic membranes thus produced were allowed to cool to room temperature before performing any characterization such as hydraulic permeability, average pore size and average porosity.

2.3 Characterization of Low Cost Ceramic Membranes

2.3.1 Determination of Hydraulic Permeability

In order to determine the hydraulic permeability, the disc-shaped ceramic membranes were first compacted using a permeability setup which consists of a pressure gauge attached to it and the apparatus was connected to an air compressor in order to maintain the setup at a particular pressure during permeation experiments. The compaction experiment involves passing water through the membrane at 206.84 kPa continuously until the time required to empty the water inside the setup (320 mL (chamber volume)) becomes constant. Following this, the time required at 137.90 kPa and 68.95 kPa were also noted. Membrane flux were then determined at the said trans-membrane pressures using the following flux-time equation (Chakraborty et al.):

$$J = \frac{V}{A \times t} \tag{1}$$

where, J, V, A, and t are the pure water flux, volume of water (or chamber), effective membrane surface area of the permeation, and time of water discharge, respectively.

The hydraulic permeability (L) of the membranes were then determined using the slope of equation (2) in accordance with the pure water flux (J) and trans-membrane pressure (ΔP) plot.

$$J = L \times \Delta P \tag{2}$$

2.3.2 Determination of Average Porosity

Archimedes' principle was used for the determination of average porosity of the membranes. Firstly, dry weights of the membrane were noted. Following which they were dipped in water for 24 h at room temperature. After 20 h, the wet weight of the membranes were measured and their average porosities were then determined using the following equation (Bose and Das, 2013):

$$\varepsilon = \frac{(w_2 - w_1) \big/ \rho_w}{\pi \times \left(D \big/ 2\right)^2 \times T} \tag{3}$$

where, ε, T, and, D are the average porosity, thickness, and disc diameter, respectively; w_1, and w_2 are the dry and wet weights of the membranes, respectively; and ρ_w is the density of water.

2.3.3 Determination of Average Pore Size

Using the hydraulic permeability and average porosity data, the average pore size of the ceramic membranes were determined according to equation (4), which was deduced based on the assumption that the membranes have cylindrical pores (Chakraborty et al.).

$$d = \left(\frac{32 \times \mu_w \times T \times L}{\varepsilon} \right)^{0.5} \quad (4)$$

where, d, ε, T, L, and μ_w are the average pore size, average porosity, thickness and permeability of the membranes, and viscosity of water, respectively.

2.4 Development of Empirical Models

The effect of the variation in interdependent variables (precursor composition) on the dependent variables, namely, average pore size and average porosities were studied by developing empirical models using Generalized Reduced Gradient (GRG) method of the MS Excel solver. Different types of models such as linear, quadratic, cubic, polyratio, and Michaelis-Menten equations as well as combination of two or more models were investigated and the best fit model to represent the dependent variables were determined. The models having highest R^2 and lowest sum of the square of errors were considered to be the best fit model. The error value was evaluated using the following formula:

$$E = \sum \left(\left(\frac{Var_{exp} - Var_{pred}}{Var_{exp}} \right) \times 100 \right)^2 \quad (5)$$

where, E, Var_{exp}, and Var_{pred} are the error, experimental values of the variables and predicted values of the variables, respectively.

2.5 Membrane Morphology

For few fabricated membranes, morphological and theoretical pore size analyses were carried out using field emission scanning electron microscopy (FESEM) (Make: Zeiss, Model: Sigma 300) and ImageJ software respectively. Thereafter, the pore sizes obtained from image analysis and experimental investigations (hydraulic permeability) were being compared.

3. Results and Discussions

3.1 Pure Water Flux

Figure 1 represents the pure water flux of VCM1 – VCM6 membranes. For all cases, the fluxes increased linearly with pressure. However, prominent variations do exist due to variation in precursor composition. The highest flux of 1.28 – 3.58 × 10^{-4} ($m^3.m^{-2}.s^{-1}$) was obtained for VCM4 membrane. The lowest flux of 6.89 × 10^{-7} – 0.18 × 10^{-7} was obtained for VCM6 membrane. All other membrane pure water flux were in similar range but not for VCM5, whose values are marginally lower than those obtained for other membranes. The membrane VCM4 was fabricated with zero feldspar content and with higher fluxes, the membrane indicates larger combinations of pore size and porosity of the membrane. Membranes VCM1, VCM2 and VCM3 exhibited similar pure water flux trends ranging from 1.05 – 3.78 × 10^{-4} ($m^3.m^{-2}.s^{-1}$).

In this regard, it shall be noted that the binder composition (sodium metasilicate and boric acid) was kept 10 wt.% for each binder in VCM1 – VCM4 membranes and was increased to 12.5 wt.% and 15 wt.% each for VCM5 and VCM6 respectively. With enhanced binder composition, membrane pure water flux values reduced significantly. Upon sintering, the binders facilitate increased bonding between precursor materials and provide greater strength to the membrane structure. A significant reduction in pure water flux for the VCM5 and VCM6 membranes affirms that the binders play a significant role in varying the membrane properties and hence the flux data.

3.2 Average Porosity

The average porosity plot followed trends similar to that of the pure water fluxes reported in the previous sub-section. Figure 2 depicts the porosity variation for various membrane samples. The maximum and minimum porosity of 30.43 and 14.08 % were obtained for VCM4 and VCM6 membranes respectively. For VCM5 membrane, an average porosity of 17.89 % was obtained which is marginally higher than that of VCM6. Thus, it is apparent that compared to

feldspar content, higher kaolin content enabled higher porosities. Higher porosities also indicate lower strength of the membrane material. Since sawdust composition was kept fixed for the investigations conducted with VCM1 – VCM4 membranes, it can be assumed that its role is negligible to alter the evaluated porosity trends. On the other hand, the binder composition can be analyzed to be significant to influence the porosity. Both kaolin and feldspar content had contrasting effect on the average membrane porosity. Among these, kaolin had more positive influence on the membrane porosity. Among the membranes, kaolin content was maximum for VCM4 membrane and followed decreased trend in the order of VCM1, VCM3 and VCM2. Kaolin is well known for its plasticity towards the membrane. On the contrary, feldspar contributes towards bonding of the materials. Thus, with increasing kaolin content, the average porosity increases and with increasing feldspar content, the average membrane porosity gets reduced.

3.3 Average Hydraulic Permeability and Average Pore Size

The hydraulic permeability and average membrane pore size trends for the membranes were similar to those reported for pure water fluxes and average porosity in the earlier sub-sections (4.2.2 and 4.2.3). Figure 3 depicts the variations of hydraulic permeability and average membrane pore size for all membranes VCM1 – VCM6. Highest combinations of hydraulic permeability and average pore size were obtained for VCM4 membrane (1.39 µm and 40.83×10^{-10} $m^3.m^{-2}.s^{-1}.Pa^{-1}$). The lowest combinations of these parameters were obtained for the VCM6 membrane (0.09 µm and 0.09×10^{-10} $m^3.m^{-2}.s^{-1}.Pa^{-1}$). Ceramic membranes VCM1, VCM2 and VCM3 possess similar pore size and hydraulic permeabilities and indicate marginal variations in their values. With increasing binder concentration, the membrane pore size varied significantly. This is due to the observation that the microfiltration membranes drifted towards nanofiltration range membranes with a significant reduction in pore size from micron range to nanometer range. For VCM5, the average pore size was 0.56 µm (560 nm). The lowest average

pore size of 0.09 μm (90 nm) was obtained for the VCM6 membrane. Hence, with minor variation in kaolin and feldspar content and with a smaller variation in binder content, significant variation in membrane properties can be targeted to broaden the scope of the membranes for wider application. For these cases, the hydraulic permeability values reduced significantly from 4.21×10^{-10} $m^3.m^{-2}.s^{-1}.Pa^{-1}$ to 0.09×10^{-10} $m^3.m^{-2}.s^{-1}.Pa^{-1}$. The lowest average pore size of 90 nm of the membrane will have a significant role in membrane fouling and hence reduced fluxes with real time applications. Such studies are to be addressed in future investigations.

An important observation among VCM1 – VCM3 membranes is that with variation in kaolin to feldspar ratio from 0.48 to 2.05, the average pore size did not vary significantly. This was not the case for porosity, with highest porosity being obtained for the case of kaolin to feldspar ratio of 0.48. These observations are anticipated to provide useful guidelines to further research upon the fabrication of low cost ceramic membranes with controlled and tailor made combinations of pore size and porosity.

3.4 Search for Best Fit Empirical Models

Similar to the empirical model fitness conducted for the earlier set of experimental data, empirical model fitness studies have been conducted for the determination of best fit model to represent pore size and porosity as functions of kaolin, feldspar and binder content. The best fit model was identified based on highest possible R^2 value of the parity plot for predicted and experimental data sets of dependent variables (pore size and porosity). The independent variables for the study refer to compositions of kaolin ([K]), feldspar ([F]), sodium metasilicate and boric acid. Since the binders (sodium metasilicate and boric acid) were taken in equal proportions for all membranes, they have been considered as a single variable ([B]).

To determine the best fit model, alternate models such as linear, quadratic, cubic, PolyRatio, Michaelis-menton, cubic, special cubic and other non-linear models have been

considered for the fitness studies. Since several independent variables are involved, it can be difficult to achieve the best fit model. Therefore, to ease the modeling effort and obtain useful insights with respect to the contribution of each composition, fitness studies were also considered by choosing a single variable at a time influencing the dependent variable. Thereby, a combination of such models has also been considered to obtain the best fit empirical model. Among all cases, highly non-linear PolyRatio model was found to be the fit model to represent the dependent variables in terms of independent variables (Equations 6 and 7). This was not the case in our earlier investigations that indicated fairly linear dependence of average pore size and non-linear dependence of porosity with respect to concentration and sawdust of the pore forming agent [26]. Relevant fitness parameters have been also presented in Table 2.

$$d_p = p + \frac{a + b[K]^{n_1}}{c + d[K]^{n_2}} + \frac{e + f[F]^{n_3}}{g + h[F]^{n_4}} + \frac{i + j[B]^{n_5}}{k + l[B]^{n_6}} \tag{6}$$

$$\varepsilon = p + \frac{a + b[K]^{n_1}}{c + d[K]^{n_2}} + \frac{e + f[F]^{n_3}}{g + h[F]^{n_4}} + \frac{i + j[B]^{n_5}}{k + l[B]^{n_6}} \tag{7}$$

It can be observed that the binders play a very important role to influence both average pore size and average porosity. This has been ascertained with the higher coefficients for the term in the modeling expression. However, the role of kaolin and feldspar are different for the both cases. For the case of porosity, the coefficients of [K] and [F] have similar influence with [F]. However, for the pore size, [F] had larger influence in comparison with [K]. Figure 4 (a) and (b) depict the parity plots of pore size and porosity determined with the best fit empirical models. The R^2 value for the porosity parity plot is 0.999 and indicates a promising trend. However, a lower but promising value of R^2 (0.959) was obtained for the average pore size parity plot. Significant scattering can be observed for the pore size case (Figure 4 (a)) in comparison with the porosity case (Figure 4 (b)). For lower average pore size, significant

variation in the predicted and measured average pore size is apparent. The model equation of pore size was found to be rather complex with larger number of coefficient terms and higher coefficient values. For lower pore size cases, complexities and interactions are likely to increase. Due to this reason, larger variation in actual vs predicted data is apparent.

3.5 Experimental and Theoretical Analysis of Membrane Morphology

Figure 5 depicts the FESEM micrographs of VCM4, VCM5 and VCM6 membranes. Based on the software based image analysis, the average pore sizes were similar to those being obtainex experimentally (1.39, 0.56 and 0.089 µm respectively. For VCM4, the theoretical pore size was obtained as 1.24 µm which is in good agreement with the experimentally determined average pore size of 1.39 µm. Similarly, for VCM5 and VCM6 membranes, the theoretical pore sizes were being evaluated as 0.58 µm and 0.097 µm, respectively. These are in good agreement with those being determined experimentally as 0.56 and 0.089 µm respectively. Further, it shall be noted that the VCM6 possessed pores in the nano-scale range and henceforth higher magnification (50 kX) was considered for comparative analysis.

3.6 Comparative Assessment of Membrane Morphological Characteristics

The low cost ceramic membrane morphological parameters obtained in this study have been compared with the most competent literature data that involved biological resources as pore forming agents. With minimal variation in other precursors and binder composition, the average pore size obtained was 0.09 µm. The literature reported lowest pore size is about 0.23 µm that was achieved with potato starch as pore former but with higher porosity (44.9 %) (Table 3). Further, it needs to be observed that for all other cases that involved biological resources as pore formers, the average pore size and porosity of the membranes were significantly higher. In summary, the research findings of this work clearly demonstrate the need for utilizing waste biological resources such as sawdust in comparison with the value

added biological starch as pore former agent to successfully achieve sub-micron size pore size of the low cost ceramic membranes. This can be suitably targeted by varying the organic pore forming agent concentration and its average particle size.

4. Conclusions

In this article, the utility of waste biological resource such as sawdust as well as other precursor components have been effectively investigated with the primary objective of the pore size reduction of the low cost ceramic membranes and enhanced applications of the membranes with sub-micron pore size. In order to reduce the pore size of the membranes by varying the precursor composition, a fundamental understanding of the contribution of all precursors is required and hence experiments had been conducted by considering variable kaolin to feldspar ratio and enhanced binder content. Such precursor composition variation facilitated significant reduction in pore size (1.39 to 0.09 μm) and porosity (30.43 to 14.09 %) of the ceramic membranes. It has been observed that increasing binder composition (from 10 – 15 wt.%) had a significant influence on the average pore size of the membranes to potentially alter them from microfiltration range to ultrafiltration range. The empirical model fitness studies provided useful insights. For increased complexity associated to the variation of precursor compositions, a highly non-linear dependence with respect to variations in the precursor compositions has been inferred. Hence it is apparent that precursor compositions have a highly complex interaction mechanism to influence the average membrane pore size and porosity of the low cost ceramic membranes. Further research can be suitably targeted for the low cost ceramic membranes using other types of biological waste resources as pore forming agents. With these developments, it is anticipated that the low cost ceramic membrane applications can be suitably extended to finer microfiltration operations such as vegetable extract processing and microbial

filtration to thereby enhance the economic competitiveness of ceramic membranes in the process industries.

References

Abdullayev, A., Bekheet, M.F., Hanaor, D.A., Gurlo, A., 2019. Materials and applications for low-cost ceramic membranes. Membranes 9, 105.

Bose, S., Das, C., 2013. Preparation and characterization of low cost tubular ceramic support membranes using sawdust as a pore-former. Materials letters 110, 152-155.

Buonomenna, M.G., 2013. Membrane processes for a sustainable industrial growth. RSC advances 3, 5694-5740.

Chakraborty, S., Das, C., Uppaluri, R., 2020a. Feasibility of Low-Cost Kaolin–Based Ceramic Membranes for Organic Lagernaria siceraria Juice Production. FOOD AND BIOPROCESS TECHNOLOGY.

Chakraborty, S., Uppaluri, R., Das, C., Effect of pore former (saw dust) characteristics on the properties of sub-micron range low-cost ceramic membranes. International Journal of Ceramic Engineering & Science.

Chakraborty, S., Uppaluri, R., Das, C., 2018. Optimal fabrication of carbonate free kaolin based low cost ceramic membranes using mixture model response surface methodology. Applied Clay Science 162, 101-112.

Chakraborty, S., Uppaluri, R., Das, C., 2020b. Combinatorial optimality of membrane morphology and feedstock during microfiltration of bottle gourd juice. Innovative Food Science & Emerging Technologies, 102382.

Ciora, R., Liu, P.K., 2003. Ceramic membranes for environmental related applications. Fluid/Particle Separation Journal 15, 51-60.

DeFriend, K.A., Wiesner, M.R., Barron, A.R., 2003. Alumina and aluminate ultrafiltration membranes derived from alumina nanoparticles. Journal of membrane science 224, 11-28.

Dong, Y., Chen, S., Zhang, X., Yang, J., Liu, X., Meng, G., 2006. Fabrication and characterization of low cost tubular mineral-based ceramic membranes for micro-filtration from natural zeolite. Journal of Membrane Science 281, 592-599.

Ha, J.-H., Lee, J., Song, I.-H., Lee, S.-H., 2015. The effects of diatomite addition on the pore characteristics of a pyrophyllite support layer. Ceramics International 41, 9542-9548.

Horri, B.A., Selomulya, C., Wang, H., 2012. Characteristics of Ni/YSZ ceramic anode prepared using carbon microspheres as a pore former. international journal of hydrogen energy 37, 15311-15319.

Issaoui, M., Limousy, L., 2019. Low-cost ceramic membranes: Synthesis, classifications, and applications. Comptes Rendus Chimie 22, 175-187.

Kumar, R., Chakrabortty, S., Pal, P., 2015. Membrane-integrated physico-chemical treatment of coke-oven wastewater: transport modelling and economic evaluation. Environmental Science and Pollution Research 22, 6010-6023.

Lorente-Ayza, M.M., Sánchez, E., Sanz, V., Mestre, S., 2015. Influence of starch content on the properties of low-cost microfiltration ceramic membranes. Ceramics International 41, 13064-13073.

Mallada, R., Menéndez, M., 2008. Inorganic membranes: synthesis, characterization and applications. Elsevier.

Mestre, S., Gozalbo, A., Lorente-Ayza, M., Sánchez, E., 2019. Low-cost ceramic membranes: A research opportunity for industrial application. Journal of the European Ceramic Society 39, 3392-3407.

Mingyi, L., Bo, Y., Jingming, X., Jing, C., 2010. Influence of pore formers on physical properties and microstructures of supporting cathodes of solid oxide electrolysis cells. International journal of hydrogen energy 35, 2670-2674.

Mohanta, K., Kumar, A., Parkash, O., Kumar, D., 2014a. Low cost porous alumina with tailored microstructure and thermal conductivity prepared using rice husk and sucrose. Journal of the American Ceramic Society 97, 1708-1719.

Mohanta, K., Kumar, A., Parkash, O., Kumar, D., 2014b. Processing and properties of low cost macroporous alumina ceramics with tailored porosity and pore size fabricated using rice husk and sucrose. Journal of the European Ceramic Society 34, 2401-2412.

Nandi, B., Uppaluri, R., Purkait, M., 2010. Microfiltration of stable oil-in-water emulsions using kaolinbased ceramic membrane and evaluation of fouling mechanism. Desalination and Water Treatment 22, 133-145.

Nandi, B., Uppaluri, R., Purkait, M., 2011. Identification of optimal membrane morphological parameters during microfiltration of mosambi juice using low cost ceramic membranes. LWT-Food Science and Technology 44, 214-223.

Obada, D.O., Dodoo-Arhin, D., Dauda, M., Anafi, F.O., Ahmed, A.S., Ajayi, O.A., 2017. Physico-mechanical and gas permeability characteristics of kaolin based ceramic membranes prepared with a new pore-forming agent. Applied Clay Science 150, 175-183.

Qin, G., Lü, X., Wei, W., Li, J., Cui, R., Hu, S., 2015. Microfiltration of kiwifruit juice and fouling mechanism using fly-ash-based ceramic membranes. Food and Bioproducts Processing 96, 278-284.

Vasanth, D., Pugazhenthi, G., Uppaluri, R., 2013. Performance of low cost ceramic microfiltration membranes for the treatment of oil-in-water emulsions. Separation Science and Technology 48, 849-858.

Wang, Y.H., Tian, T.F., Liu, X.Q., Meng, G.Y., 2006. Titania membrane preparation with chemical stability for very hash environments applications. Journal of membrane science 280, 261-269.

Xavier, L.A., de Oliveira, T.V., Klitzke, W., Mariano, A.B., Eiras, D., Vieira, R.B., 2019. Influence of thermally modified clays and inexpensive pore-generating and strength improving agents on the properties of porous ceramic membrane. Applied Clay Science 168, 260-268.

Yang, G.C., Tsai, C.-M., 2008. Effects of starch addition on characteristics of tubular porous ceramic membrane substrates. Desalination 233, 129-136.

Table 1: Summary of membranes targeted through variant precursor compositions.

S. No.	Composition (wt. %)				Nomenclature
	Kaolin	Feldspar	Boric Acid	Sodium Metasilicate	
1	48.18	23.60	10	10	VCM1
2	23.60	48.18	10	10	VCM2
3	35.90	35.9	10	10	VCM3
4	71.81	0	10	10	VCM4
5	41.88	24.92	12.5	12.5	VCM5
6	38.77	23.03	15	15	VCM6

Table 2: Best fit empirical models and their parameters to represent average pore size

Model Coefficients	Pore Size (d_p) (µm)	Porosity (ε) (%)
p	1×10^{-6}	1×10^{-6}
a	0.8729	1×10^{-6}
b	0.6624	0.0111
c	1.0072	4.1785
d	1.5450	4.5319
e	18.5916	1×10^{-6}
f	0.1487	1.1079
g	48.4956	5.3013
h	4.0417	0.0021
i	40318.89	9.2167
j	5824.605	8.8252
k	28623.22	1×10^{-6}
l	1×10^{-6}	0.0001
n_1	1×10^{-6}	2.3751
n_2	5.1454	0.2946
n_3	2.8050	2.5104
n_4	29.1949	3.9675
n_5	1×10^{-6}	1×10^{-6}
n_6	2.8708	2.9784
R^2	0.959	0.999

Table 3: Data summary of ceramic membranes fabricated with low cost precursors.

S. No.	Pore Former	Other Precursors (wt.%)	Pore Size (µm)	Porosity (%)	References
1	Corn Starch Quantity: 0-15 wt.% Average Particle Size: 53 µm	• Alumina: 75 – 90 • Bentonite: 10	1 – 2.1	23.44 – 43.96	(Yang and Tsai, 2008)
2	Cationic manioc starch (CMS) grade Superion 300 Quantity: 0 – 15 wt.% Average Particle Size: 23.26 µm	• Egg Shell: 0 – 15 • Water: 10 • Natural Clay: 75 – 85	–	35.50 – 56.30	(Xavier et al., 2019)
3	Potato Starch Quantity: 0 – 30 wt.%	• Kaolin: 35 – 50 • Alumina: 35 – 50	0.23 – 2.35	44.9 – 67.3	(Lorente-Ayza et al., 2015)
4	Rice Husk Quantity: 5 – 40 wt.% Average Particle Size: 75 – 600 µm	• Sucrose: 20 • Alumina: 40 – 75	Fine pores: 4 µm Interconnected Pores: 50 – 516 µm (length)	20 – 66	(Mohanta et al., 2014a)
5	Sawdust Quantity: 8 wt.% Average Particle Size: 254 µm	• Kaolin: 38.77 – 71.18 • Feldspar: 0 – 48.18 • Sodium Metasilicate: 10 – 15 • Boric Acid: 10 – 15	0.09 – 1.39	14.09 – 30.43	This Work

List of Figures

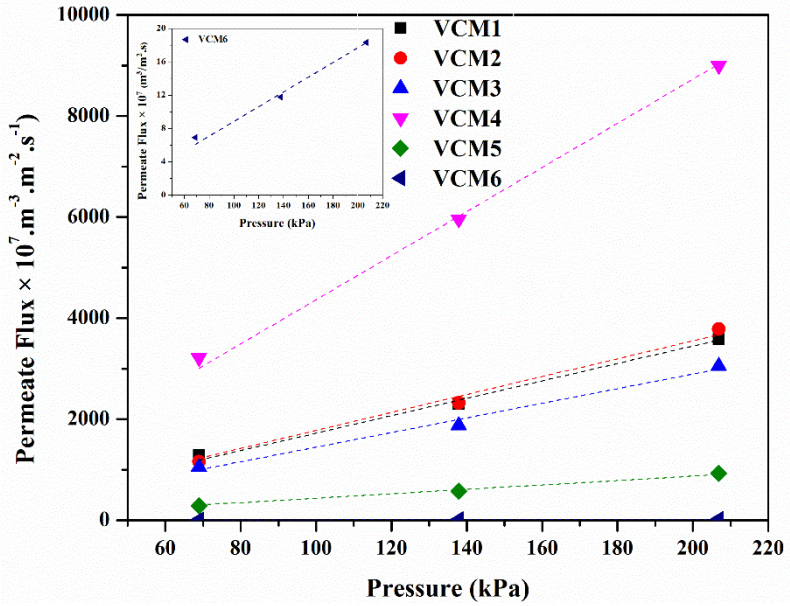

Figure 1: Pure water flux plot of alternate membranes fabricated with variant precursor compositions.

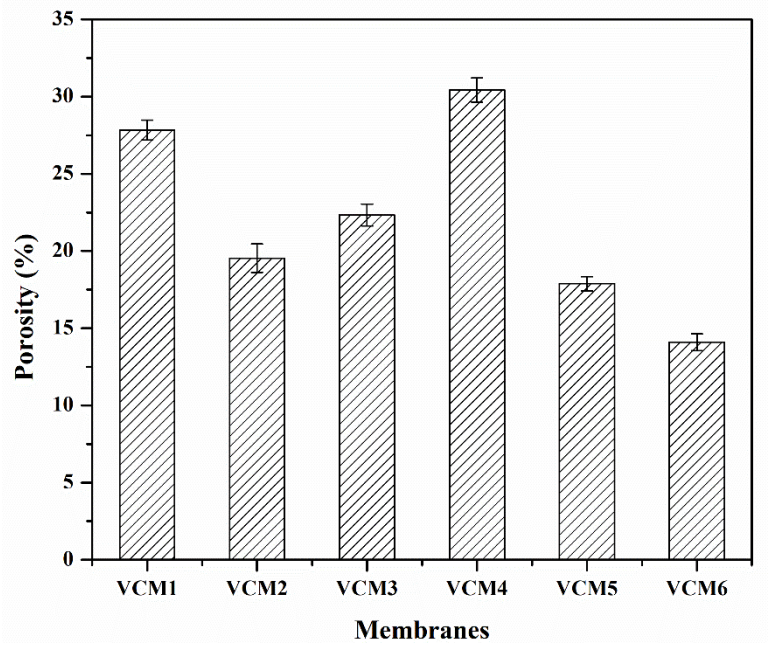

Figure 2: Average porosity characteristics of membranes fabricated with variant precursor compositions.

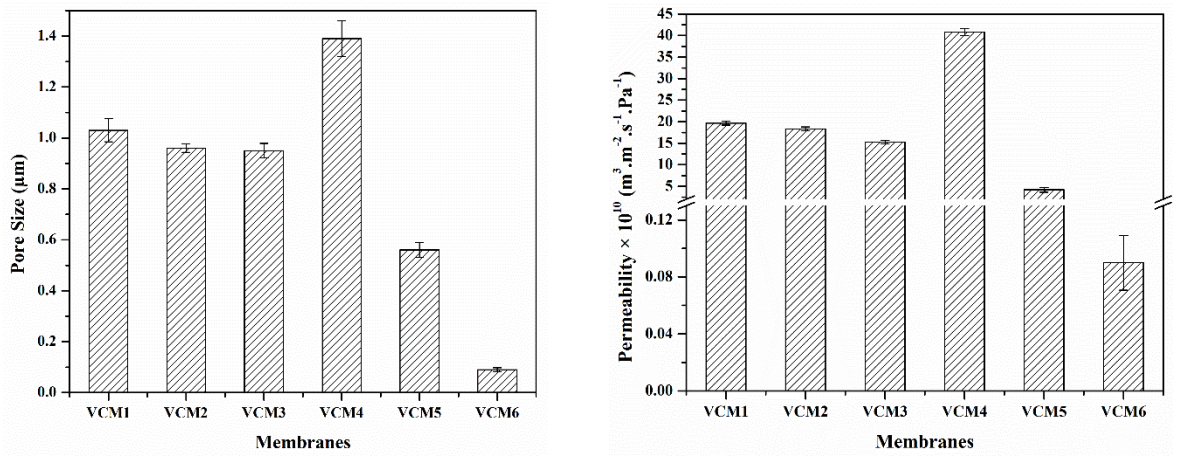

(a) **(b)**

Figure 3: Morphological characteristics of membranes fabricated with variant precursor compositions (a) average hydraulic permeability, and (b) average pore size.

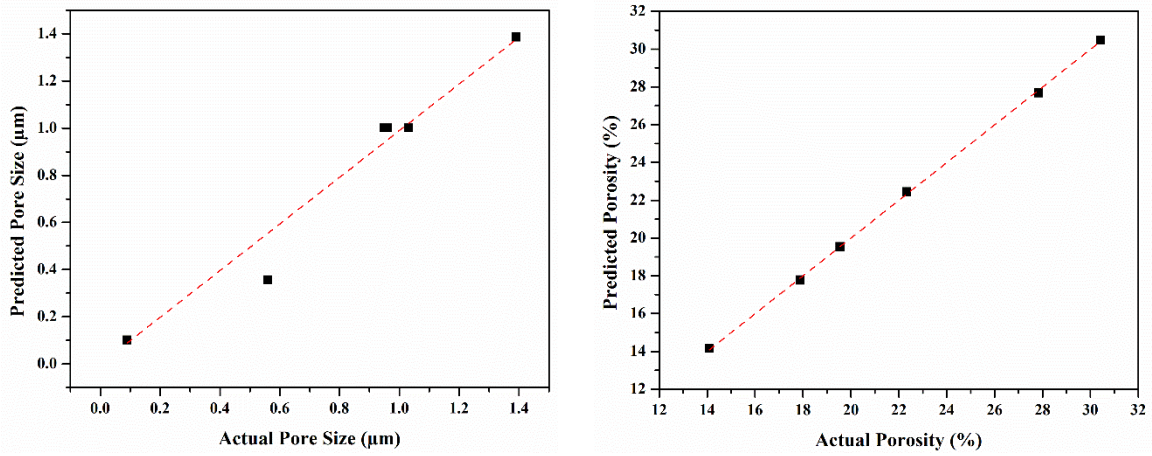

(a) **(b)**

Figure 4: Parity plot of morphological characteristics of VCM1 – VCM6 membranes (a) average pore size, and (b) average porosity.

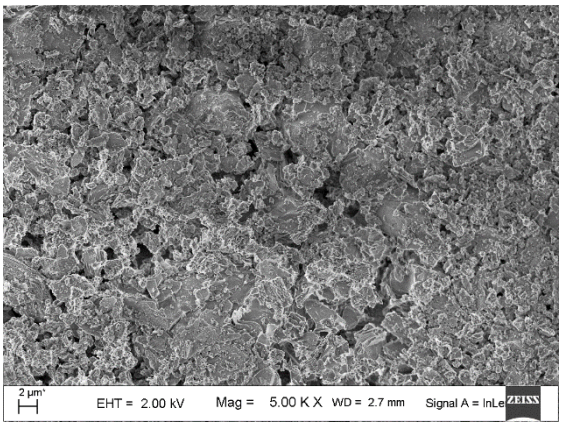

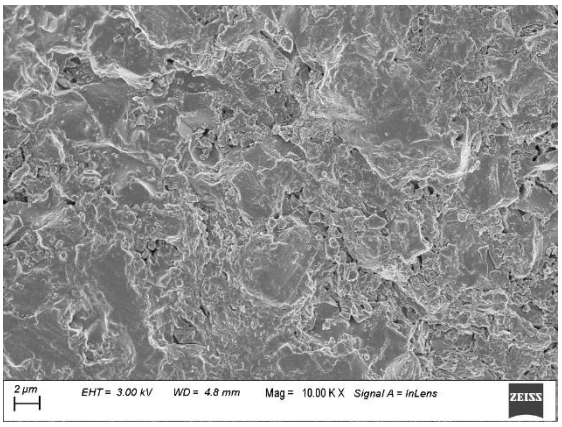

(a) **(b)**

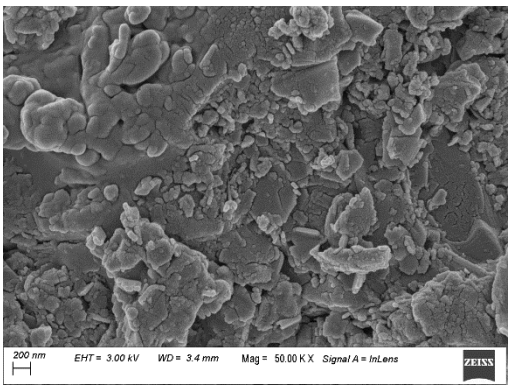

(c)

Figure 5: FESEM micrographs of (a) VCM4, (b) VCM5, and (c) VCM6 membranes.

Figures

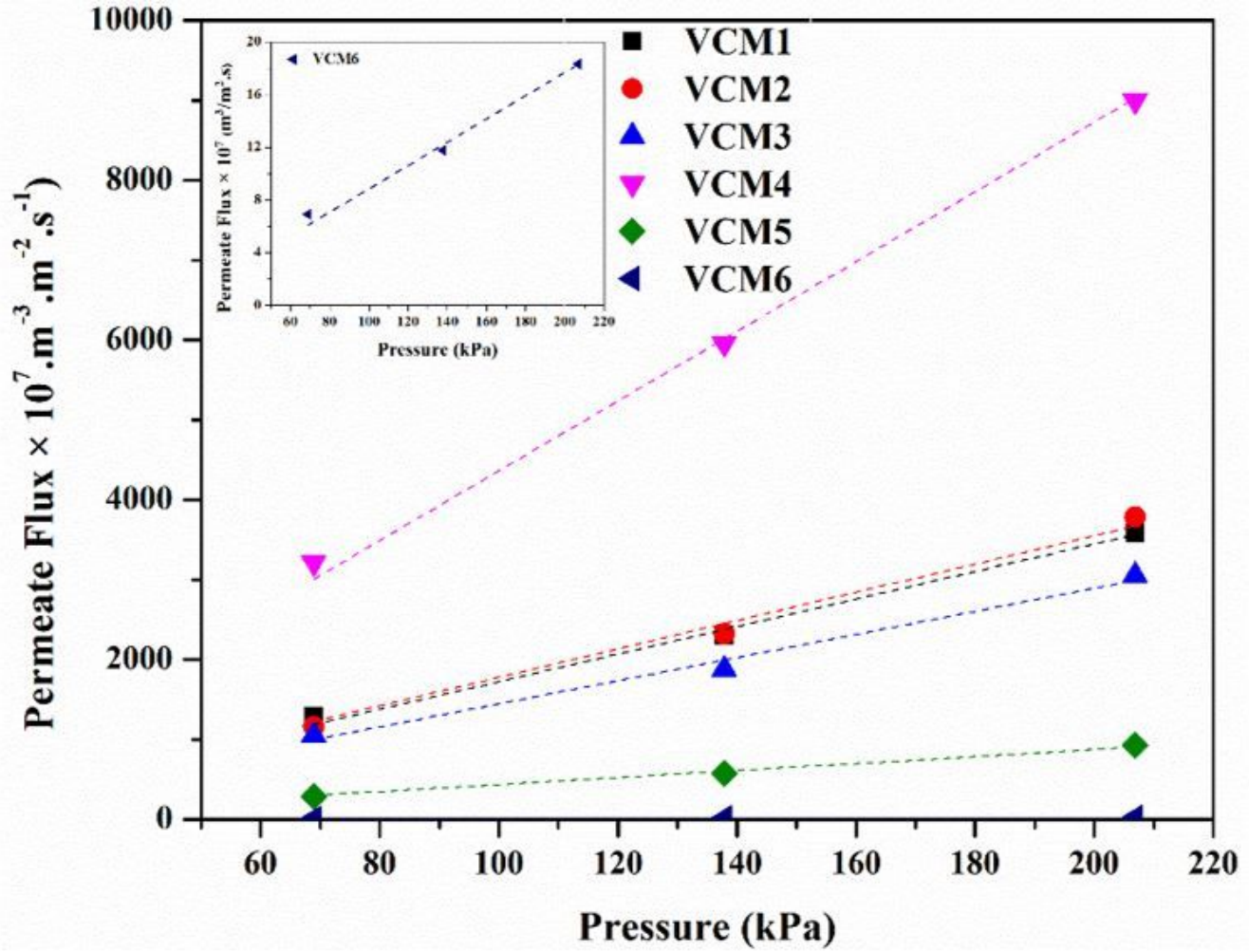

Figure 1

Pure water flux plot of alternate membranes fabricated with variant precursor compositions.

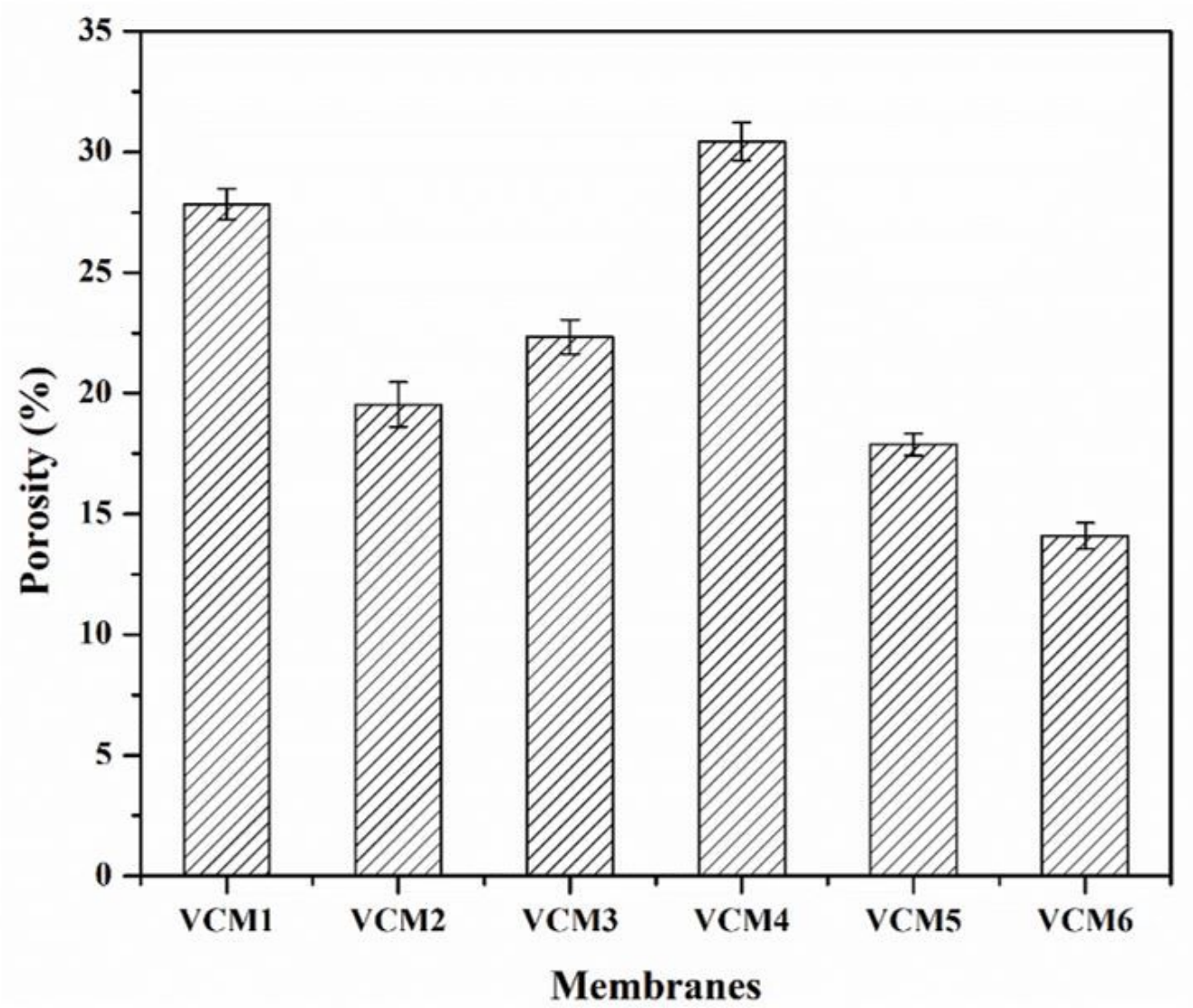

Figure 2

Average porosity characteristics of membranes fabricated with variant precursor compositions.

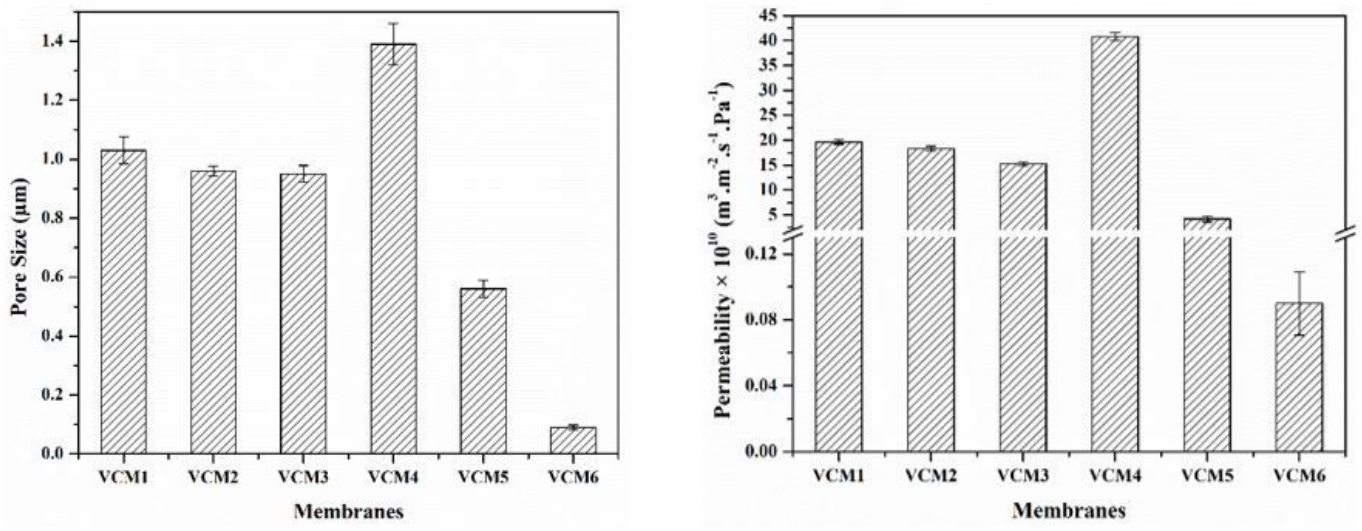

Figure 3

Morphological characteristics of membranes fabricated with variant precursor compositions (a) average hydraulic permeability, and (b) average pore size.

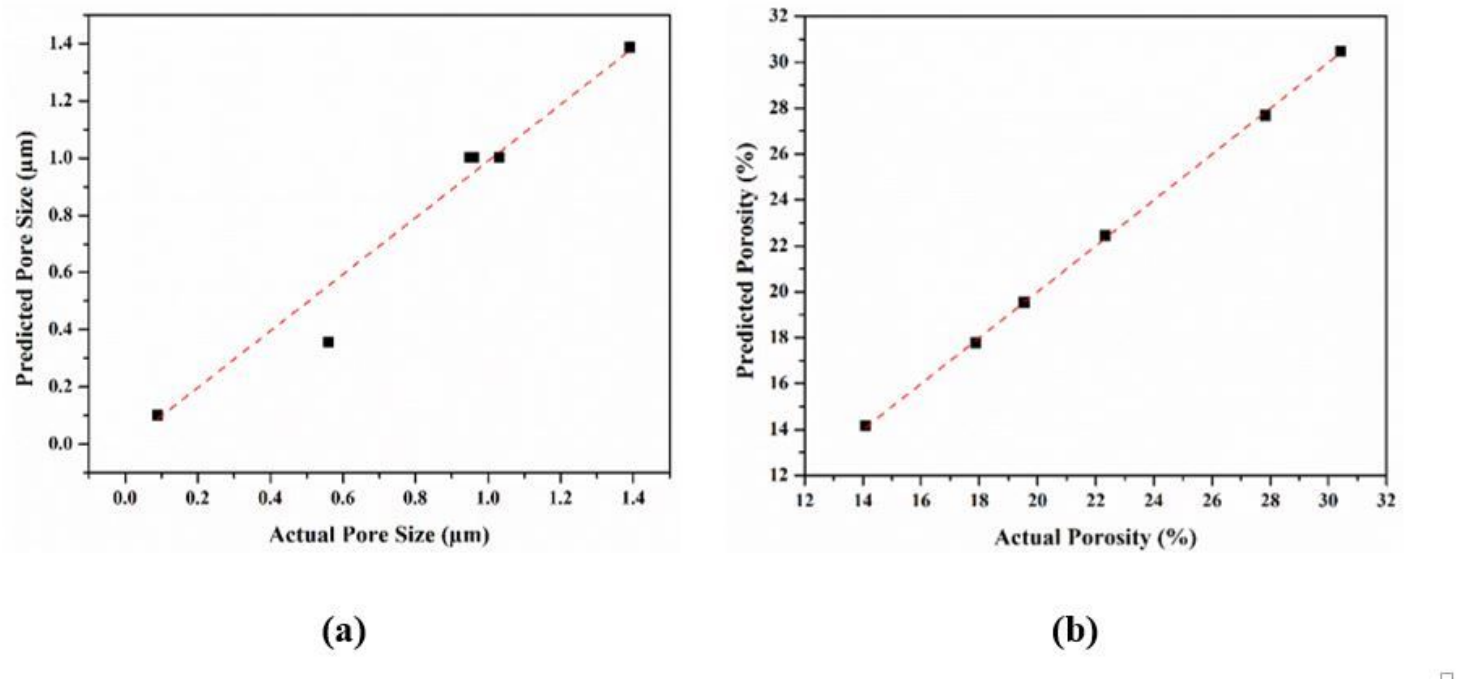

Figure 4

Parity plot of morphological characteristics of VCM1 – VCM6 membranes (a) average pore size, and (b) average porosity.

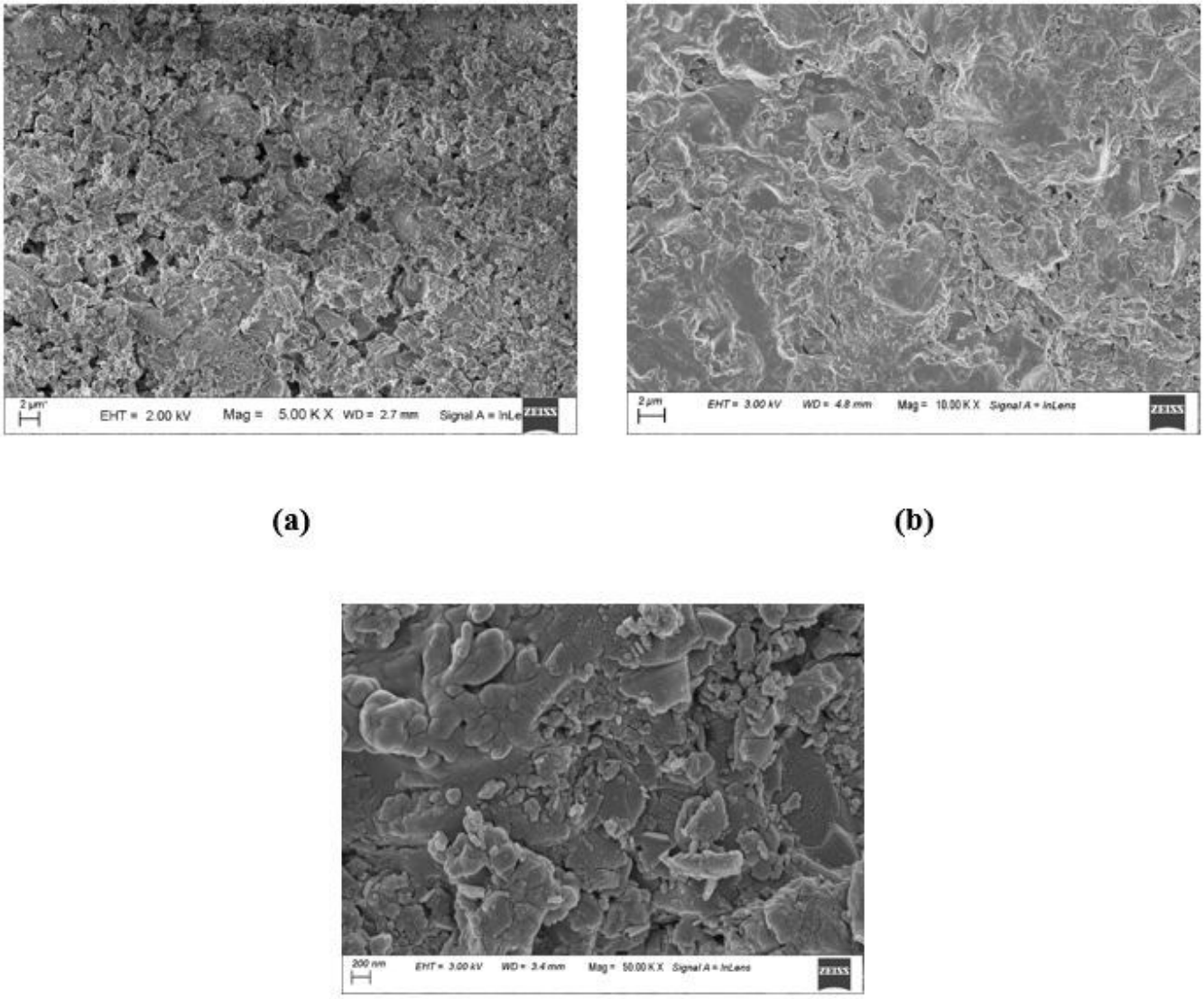

Figure 5

FESEM micrographs of (a) VCM4, (b) VCM5, and (c) VCM6 membranes.